Available online at www.sciencedirect.com
ScienceDirect
Journal of Sound and Vibration 323 (2009) 718–736
JOURNAL OF SOUND AND VIBRATION
www.elsevier.com/locate/jsvi

Improved substructuring method for eigensolutions of large-scale structures

Shun Weng[a,1], Yong Xia[a,*], You-Lin Xu[a,2], Xiao-Qing Zhou[b,3], Hong-Ping Zhu[c,4]

[a]*Department of Civil & Structural Engineering, The Hong Kong Polytechnic University, Hung Hom, Kowloon, Hong Kong*
[b]*Maunsell Structural Consultants Ltd., 138 Shatin Rural Committee Road, Shatin, Hong Kong*
[c]*School of Civil Engineering & Mechanics, Huazhong University of Science and Technology, Wuhan, Hubei, PR China*

Received 5 May 2008; received in revised form 18 December 2008; accepted 6 January 2009
Handling Editor: J. Lam
Available online 18 February 2009

Abstract

The substructuring technology possesses much merit when it is utilized in model updating or damage identification of large-scale structures. However, the conventional substructuring technologies require the complete eigensolutions of all substructures available to obtain the eigensolutions of the global structure, even if only a few eigensolutions of the global structure are needed. This paper proposes a modal truncation approximation in substructuring method, in which only the lowest eigensolutions of the substructures need to be calculated. Consequently, the computation efficiency is improved. The discarded higher eigensolutions are compensated by the residual flexibility. The division of substructures and the selection of master modes in each substructure are also studied. The proposed substructuring method is illustrated by a frame structure and a practical bridge. The two case studies verify that the proposed method can improve the original substructuring method significantly.

1. Introduction

In recent decades, finite element (FE) model updating technique has been widely developed in aerospace, mechanical and civil engineering. During FE model updating process, elemental parameters in the FE model are iteratively modified, so that the modal properties (such as frequencies and mode shapes) match the measured counterparts in an optimal way [1]. To achieve this, the eigensolutions and the sensitivity matrix of the analytical model need to be calculated repeatedly [2]. When tackling large-scale structures, three major difficulties arise. Firstly, since the analytical model of a large-scale structure consists of many degrees of

*Corresponding author. Tel.: +852 2766 6066; fax: +852 2334 6389.
E-mail addresses: 06901937r@polyu.edu.hk (S. Weng), ceyxia@polyu.edu.hk (Y. Xia), ceylxu@polyu.edu.hk (Y.-L. Xu), xq.zhou@maunsell.aecom.com (X.-Q. Zhou), hpzhu@mail.hust.edu.cn (H.-P. Zhu).
[1]Tel.: +852 2766 4485; fax: +852 2334 6389.
[2]Tel.: +852 2766 6050; fax: +852 2334 6389.
[3]Tel.: +852 3562 6485; fax: +852 2317 7609.
[4]Tel.: +85 27 87542631.

0022-460X/$ - see front matter © 2009 Elsevier Ltd. All rights reserved.
doi:10.1016/j.jsv.2009.01.015

freedom (dofs), the resulting mass matrix and stiffness matrix need very large space to store. Secondly, and more importantly, the computation effort may be great in extracting the eigensolutions and sensitivity matrix from the mass and stiffness matrices, which need to be calculated repeatedly. Thirdly, the number of parameters that need to be updated in a large-scale structure can be large, which may hinder the convergence of the optimization process.

To overcome these difficulties, the substructuring method will be a good preference. Firstly, it is possible to analyze each substructure independently, or even concurrently with parallel computing [3]. While identical substructures exist, the computation load is reduced further. Secondly, when only particular substructures need to be focused on, it is more efficient to calculate the eigensolutions and sensitivity matrix of the particular substructures iteratively during the model updating process. Thirdly, the number of parameters updated in each substructure is much less than that in the global structure. This improves the convergence of model updating process. Handling smaller problems at a time can improve the accuracy of the solutions since accumulated error during the computation is reduced [4]. In addition, the substructuring method is potentially advantageous when applied together with model reduction technique. Most model reduction methods usually take up a large amount of computation time for the construction of the reduced system. With the substructuring method, the reduced system can be constructed based on the substructures and then be assembled, so the computation load can be reduced [5,6].

When utilizing the substructuring concept in the sensitivity based model updating, it is the first step to obtain the eigensolutions via the substructuring method. Substructuring technique for the calculation of eigensolutions includes two categories, one is component mode synthesis and the other one is the Kron's substructuring method. The component mode synthesis method can be further classified into three groups according to the interface condition of the substructures, i.e., free-interface method [7], fixed-interface method [8,9], and hybrid method [10,11]. In component mode synthesis method, the modes of the substructures are divided into several parts, and each part needs to be calculated, respectively. Nevertheless, in the Kron's substructuring method, the boundary condition of the substructures is not required to be particularly considered.

Kron firstly proposed a substructuring method in the book *Diakoptics* [12] to study the eigensolutions of the systems with a very large number of variables in a piecewise manner. It constituted the receptance matrix by imposing displacement constraints at the tearing coordinates of the adjacent substructures via the Lagrange multiplier technique and virtual work theorem. Simpson and Tabarrok [13] initiated Kron's complicated electrical notation into its structural receptance form, and searched the eigenvalues by the bisection scanning and the sign count algorithm. Afterwards, Simpson [14] replaced the receptance form with a transcendental dynamic stiffness matrix. The Newtonian process is utilized to accelerate the computation speed. Williams and Kennedy [15] proposed a multiple determinant parabolic interpolation method to ensure the successful convergence on the required eigenvalues in all circumstances, and further improved the Simpson's Newtonian method [14]. Lui [16] discussed some theoretical aspects of the Kron's receptance matrix, such as the zeros and poles of the eigenvalues, and summarized detailed characteristics of the Kron's substructuring method.

Sehmi analyzed the Kron's receptance matrix with numerical solution, such as Subspace Iteration method [17] and Lanczos method [18]. Mackenzie [19] validated this substructuring method and showed that the in-core requirements and operational counts were very competitive when Subspace Iterative and Lanczos techniques were introduced.

In Kron's substructuring method, it is indispensable to evaluate the contribution of the complete eigensolutions of all substructures when assembling the primitive system, i.e., calculating all eigenpairs of each substructure primarily. This is onerous and time-consuming, since only the first a few eigensolutions are generally of interest for most researchers. Turner [20] attempted to reduce the computation load by static mass condensation, but the results were not precise enough to satisfy the usual requirement. Subsequently, this method was ignored by researchers, because it was not comparable to other fast eigensolvers, such as Lanczos method and Subspace Iteration method. To facilitate the substructuring-based model updating, Kron's substructuring method should be improved in terms of efficiency and accuracy.

This paper aims to improve the Kron's substructuring method to calculate the eigensolutions of the large-scale structures using modal truncation approximation. In the proposed method, only the first a few eigensolutions of each substructure need to be calculated. The discarded eigensolutions of the substructures are compensated with residual flexibility, including the first-order residual flexibility and the second-order

residual flexibility. The improvement on the efficiency and accuracy of the proposed substructuring method is illustrated by a frame structure and a practical bridge structure. The results demonstrate that the proposed method can reduce computation load while achieving high precision.

2. Basic theorem of substructuring method

For a global structure with N dofs, its stiffness matrix and mass matrix will be order of $N \times N$. Application of the substructuring method firstly requires that the global structure is torn or divided into NS independent substructures [21], and each substructure has n_j dofs ($j = 1,2,\ldots,NS$). This division procedure will produce NT tearing dofs. Each one tearing dof will become into two or more dofs after division, i.e. a tearing dof in the original global structure is shared by two or more substructures that are connected to it. The total number of dofs of all substructures will be expanded to NP, which is larger than N.

If the mth ($m = 1,2,\ldots,NT$) tearing dof is shared by t_m substructures, one has

$$NP = N + \sum_{m=1}^{NT}(t_m - 1), \quad NP = \sum_{j=1}^{NS} n_j \tag{1}$$

To be viewed as an independent structure, each substructure has its stiffness matrix $\mathbf{K}^{(j)}$ and mass matrix $\mathbf{M}^{(j)}$ ($j = 1,2,\ldots,NS$). The generalized eigen-equation of the jth substructure can be written as

$$\mathbf{K}^{(j)}\{\phi_i^{(j)}\} = \lambda_i^{(j)}\mathbf{M}^{(j)}\{\phi_i^{(j)}\} \tag{2}$$

both the stiffness matrix $\mathbf{K}^{(j)}$ and the mass matrix $\mathbf{M}^{(j)}$ are of order $n_j \times n_j$. $\lambda_i^{(j)}$and $\{\phi_i^{(j)}\}$ are the ith eigenvalue and eigenvector of the jth substructure, respectively. Eq. (2) yields n_j eigenvalues $\mathbf{\Lambda}^{(j)} = \mathrm{Diag}[\lambda_1^{(j)}, \lambda_2^{(j)}, \ldots, \lambda_{n_j}^{(j)}]$, and the corresponding eigenvectors $\mathbf{\Phi}^{(j)} = [\phi_1^{(j)}, \phi_2^{(j)}, \ldots, \phi_{n_j}^{(j)}]$.

With mass normalization, one has

$$\begin{cases} [\mathbf{\Phi}^{(j)}]^{\mathrm{T}}\mathbf{M}^{(j)}\mathbf{\Phi}^{(j)} = \mathbf{I}_{n_j} \\ [\mathbf{\Phi}^{(j)}]^{\mathrm{T}}\mathbf{K}^{(j)}\mathbf{\Phi}^{(j)} = \mathbf{\Lambda}^{(j)} \end{cases} \tag{3}$$

Diagonal assembling the substructures to the primitive form gives

$$\mathbf{M}^p = \mathrm{Diag}[\mathbf{M}^{(1)}, \mathbf{M}^{(2)}, \ldots, \mathbf{M}^{(NS)}] \quad \mathbf{K}^p = \mathrm{Diag}[\mathbf{K}^{(1)}, \mathbf{K}^{(2)}, \ldots, \mathbf{K}^{(NS)}]$$

$$\mathbf{\Phi}^p = \mathrm{Diag}[\mathbf{\Phi}^{(1)}, \mathbf{\Phi}^{(2)}, \ldots, \mathbf{\Phi}^{(NS)}] \quad \mathbf{\Lambda}^p = \mathrm{Diag}[\mathbf{\Lambda}^{(1)}, \mathbf{\Lambda}^{(2)}, \ldots, \mathbf{\Lambda}^{(NS)}] \tag{4}$$

where superscript 'p' denotes the variables associated with the primitive form, and the size of the above matrices is $NP \times NP$. Due to the orthogonality conditions in Eq. (3), it follows that:

$$\begin{cases} [\mathbf{\Phi}^p]^{\mathrm{T}}\mathbf{M}^p\mathbf{\Phi}^p = \mathbf{I}_{NP} \\ [\mathbf{\Phi}^p]^{\mathrm{T}}\mathbf{K}^p\mathbf{\Phi}^p = \mathbf{\Lambda}^P \end{cases} \tag{5}$$

Reconnection of the primitive system can be performed by considering the geometric compatibility and force equilibrium at the tearing points of the adjacent substructures. If $\{x\}$ is the displacement vector of the original global structure with the size of $N \times 1$, it can be expanded to $\{\overline{x}\}$ with the size of $NP \times 1$ after substructuring, which includes identical displacements in the tearing dofs. The geometric compatibility is enforced by applying displacement constraints as

$$\mathbf{C}\{\overline{x}\} = 0 \tag{6}$$

$\mathbf{C}$ is a rectangular matrix which contains general implicit constraints to make sure the nodes at the interface have identical displacement, which is described in Appendix A.

With the virtual work theorem, the motion equation of the undamped structure is

$$\mathbf{M}^p\{\ddot{\overline{x}}\} + \mathbf{K}^p\{\overline{x}\} = \mathbf{F}_{\mathrm{ext}} + \mathbf{F}_{\mathrm{con}} \tag{7}$$

For a free vibration system, external excitation force $\mathbf{F}_{ext} = 0$, and the virtual work done by the connection forces $\mathbf{F}_{con}$ along $\{\overline{x}\}$ is

$$\delta \mathbf{W} = \mathbf{F}_{con}^{T}\{\delta \overline{x}\} \tag{8}$$

Considering the connection process to be incomplete, the compatibility is violated at the tearing coordinates by an amount of $\{\eta\}$. Eq. (6) becomes

$$\mathbf{C}\{\overline{x}\} = \{\eta\} \tag{9}$$

In the new coordinates there will be an associated force vector $\{\tau\}$, representing the internal connection forces due to the 'misfit'. Combination of Eqs. (8) and (9) gives

$$\delta \mathbf{W} = \{\tau\}^{T}\{\delta\eta\} = \{\tau\}^{T}\mathbf{C}\{\delta \overline{x}\} \tag{10}$$

From Eqs. (8) and (10), one can obtain

$$\mathbf{F}_{con}^{T}\{\delta \overline{x}\} = \{\tau\}^{T}\mathbf{C}\{\delta \overline{x}\} \tag{11}$$

It is obvious that

$$\mathbf{F}_{con} = \mathbf{C}^{T}\{\tau\} \tag{12}$$

Consequently, Eq. (7) can be transformed into

$$\begin{bmatrix} \mathbf{M}^{p} & \mathbf{0} \\ \mathbf{0} & \mathbf{0} \end{bmatrix} \begin{Bmatrix} \ddot{\overline{x}} \\ \ddot{\tau} \end{Bmatrix} + \begin{bmatrix} \mathbf{K}^{p} & -\mathbf{C}^{T} \\ -\mathbf{C} & \mathbf{0} \end{bmatrix} \begin{Bmatrix} \overline{x} \\ \tau \end{Bmatrix} = \begin{Bmatrix} \mathbf{0} \\ \mathbf{0} \end{Bmatrix} \tag{13}$$

Assuming the oscillatory solution of the form $\{\overline{x}, \tau\}^{T} = \{\overline{\phi}, \tau\}^{T} \exp(i\sqrt{\overline{\lambda}}t)$, the expanded mode shape of the global structure can be related to the primitive form of the mode shapes $\mathbf{\Phi}^{p}$ via the modal coordinates $\mathbf{z}$ as [22]

$$\begin{Bmatrix} \overline{\phi} \\ \tau \end{Bmatrix} = \begin{bmatrix} \mathbf{\Phi}^{p} & \mathbf{0} \\ \mathbf{0} & \mathbf{I} \end{bmatrix} \begin{Bmatrix} \mathbf{z} \\ \tau \end{Bmatrix} \tag{14}$$

where $\overline{\phi}$ is the expanded mode shape of the global structure including identical values in the interface dofs. Considering the orthogonality relations in Eq. (5), Eq. (13) can be transformed into the canonical form

$$\begin{bmatrix} \mathbf{\Lambda}^{p} - \overline{\lambda}\mathbf{I} & -\mathbf{\Gamma} \\ -\mathbf{\Gamma}^{T} & \mathbf{0} \end{bmatrix} \begin{Bmatrix} \mathbf{z} \\ \tau \end{Bmatrix} = \begin{Bmatrix} \mathbf{0} \\ \mathbf{0} \end{Bmatrix} \tag{15}$$

where $\mathbf{\Gamma} = (\mathbf{C}\mathbf{\Phi}^{p})^{T}$ is referred to as the normal connection matrix. With the above-described procedure, the nodes at the tearing points of the adjacent structures are constrained to move jointly. Therefore, the eigenvalue $\overline{\lambda}$ obtained with Eq. (15) is equal to the eigenvalue λ belonging to the original global structure. If $\bar{\mathbf{\Phi}}$consists of the expanded eigenvectors $\overline{\phi}$, the eigenvectors of the global structure $\mathbf{\Phi}$ can be obtained after discarding the identical dofs in $\bar{\mathbf{\Phi}}$. $\mathbf{\Gamma}$ has the order of $NP \times (NP - N)$, where $(NP-N)$ is the number of constraint relations and much less than NP.

The first equation of Eq. (15) gives

$$\mathbf{z} = (\mathbf{\Lambda}^{p} - \overline{\lambda}\mathbf{I})^{-1}\mathbf{\Gamma}\tau \tag{16}$$

Substituting Eq. (16) into the second equation of Eq. (15) to eliminate the modal coordinates $\mathbf{z}$, one has

$$\mathbf{\Gamma}^{T}(\mathbf{\Lambda}^{p} - \overline{\lambda}\mathbf{I})^{-1}\mathbf{\Gamma}\tau = 0 \quad \text{or } \mathbf{R}\tau = 0 \tag{17}$$

in which $\mathbf{R} = \mathbf{\Gamma}^{\mathbf{T}}\mathbf{D}\mathbf{\Gamma}$ and $\mathbf{D} = (\mathbf{\Lambda}^{p} - \overline{\lambda}\mathbf{I})^{-1}$.

The matrix $\mathbf{R}$ with size of $(NP - N) \times (NP - N)$, is known as the *Kron matrix* or *receptance matrix* [17]. Since the above analysis has no approximation in the derivation of $\mathbf{R}$, the eigenvalues obtained will be identical to the initial structural idealizations made in the FE modeling of the global structure.

$\overline{\lambda}$ is obtained by scanning $\mathbf{R}$'s determinant in the original Kron's method [23]. Obviously, this is very time-consuming since $\mathbf{R}$ is dependent on the unknown $\overline{\lambda}$ [24]. Sehmi [17,18] applied numerical approaches (Subspace Iteration method and Lanczos method) to the Kron's substructuring method, and estimated the

eigensolutions more efficiently. Nevertheless, it is onerous to calculate the complete eigensolutions of each substructure to assemble $\mathbf{\Lambda}^p$ and $\mathbf{\Phi}^p$. Further, the final eigen-equation for searching eigensolutions has the size of $NP \times NP$, which will be very large for large-scale structures.

To overcome this, the present paper will improve the efficiency of the Kron's substructuring method by introducing a modal truncation technique. This is based on the fact that the higher modes have little contribution to the receptance matrix. The first-order simplification will be intended firstly, followed by a second-order counterpart.

3. First-order residual flexibility based modal truncation

In each substructure, a few eigensolutions, which correspond to lower vibration modes, are selected as 'master' variables. The residual higher modes are treated as 'slave' variables. Similar to the model reduction technique [5,6,25], the masters will be retained while the slaves are discarded in the later calculations. Subscript 'm' and 's' will represent 'master' and 'slave' variables, respectively, hereinafter.

Assuming that the first m_j ($j = 1,2,\ldots,NS$) modes are chosen as the 'master' modes in the jth substructure while the residual s_j higher modes are the 'slave' modes, the jth substructure has 'master' eigenpairs and 'slave' eigenpairs as

$$\mathbf{\Lambda}_m^{(j)} = \mathrm{Diag}[\lambda_1^{(j)}, \lambda_2^{(j)}, \ldots, \lambda_{m_j}^{(j)}]$$

$$\mathbf{\Phi}_m^{(j)} = [\phi_1^{(j)}, \phi_2^{(j)}, \ldots, \phi_{m_j}^{(j)}]$$

$$\mathbf{\Lambda}_s^{(j)} = \mathrm{Diag}[\lambda_{m_j+1}^{(j)}, \lambda_{m_j+2}^{(j)}, \ldots, \lambda_{m_j+s_j}^{(j)}]$$

$$\mathbf{\Phi}_s^{(j)} = [\phi_{m_j+1}^{(j)}, \phi_{m_j+2}^{(j)}, \ldots, \phi_{m_j+s_j}^{(j)}]$$

$$m^p = \sum_{j=1}^{NS} m_j, \quad s^p = \sum_{j=1}^{NS} s_j, \;\; m_j + s_j = n_j \;\; (j = 1,2,\ldots,NS) \tag{18}$$

Assembling all 'master' eigenpairs and 'slave' eigenpairs, respectively, one has

$$\mathbf{\Lambda}_m^p = \mathrm{Diag}[\mathbf{\Lambda}_m^{(1)}, \mathbf{\Lambda}_m^{(2)}, \ldots, \mathbf{\Lambda}_m^{(NS)}]$$

$$\mathbf{\Phi}_m^p = \mathrm{Diag}[\mathbf{\Phi}_m^{(1)}, \mathbf{\Phi}_m^{(2)}, \ldots, \mathbf{\Phi}_m^{(NS)}]$$

$$\mathbf{\Lambda}_s^p = \mathrm{Diag}[\mathbf{\Lambda}_s^{(1)}, \mathbf{\Lambda}_s^{(2)}, \ldots, \mathbf{\Lambda}_s^{(NS)}]$$

$$\mathbf{\Phi}_s^p = \mathrm{Diag}[\mathbf{\Phi}_s^{(1)}, \mathbf{\Phi}_s^{(2)}, \ldots, \mathbf{\Phi}_s^{(NS)}] \tag{19}$$

Denoting $\mathbf{\Gamma}_m = [\mathbf{C}\mathbf{\Phi}_m^p]^{\mathrm{T}}$ and $\mathbf{\Gamma}_s = [\mathbf{C}\mathbf{\Phi}_s^p]^{\mathrm{T}}$, Eq. (15) can be expanded as

$$\begin{bmatrix} \mathbf{\Lambda}_m^p - \overline{\lambda}\mathbf{I} & \mathbf{0} & -\mathbf{\Gamma}_m \\ \mathbf{0} & \mathbf{\Lambda}_s^p - \overline{\lambda}\mathbf{I} & -\mathbf{\Gamma}_s \\ -\mathbf{\Gamma}_m^{\mathrm{T}} & -\mathbf{\Gamma}_s^{\mathrm{T}} & \mathbf{0} \end{bmatrix} \begin{Bmatrix} \mathbf{z}_m \\ \mathbf{z}_s \\ \tau \end{Bmatrix} = \begin{Bmatrix} \mathbf{0} \\ \mathbf{0} \\ \mathbf{0} \end{Bmatrix} \tag{20}$$

The second equation of Eq. (20) gives

$$\mathbf{z}_s = (\mathbf{\Lambda}_s^p - \overline{\lambda}\mathbf{I})^{-1}\mathbf{\Gamma}_s\tau \tag{21}$$

Substituting Eq. (21) into Eq. (20) results in

$$\begin{bmatrix} \mathbf{\Lambda}_m^p - \overline{\lambda}\mathbf{I} & -\mathbf{\Gamma}_m \\ -\mathbf{\Gamma}_m^{\mathrm{T}} & -\mathbf{\Gamma}_s^{\mathrm{T}}(\mathbf{\Lambda}_s^p - \overline{\lambda}\mathbf{I})^{-1}\mathbf{\Gamma}_s \end{bmatrix} \begin{Bmatrix} \mathbf{z}_m \\ \tau \end{Bmatrix} = \begin{Bmatrix} \mathbf{0} \\ \mathbf{0} \end{Bmatrix} \tag{22}$$

In Eq. (22), the Taylor expansion principle introduces

$$(\mathbf{\Lambda}_s^p - \overline{\lambda} I)^{-1} = (\mathbf{\Lambda}_s^p)^{-1} + \overline{\lambda}(\mathbf{\Lambda}_s^p)^{-2} + \overline{\lambda}^2(\mathbf{\Lambda}_s^p)^{-3} + \cdots \tag{23}$$

In general, the required eigenvalues $\overline{\lambda}$ correspond to the lowest modes of the global structure, and far less than the items in $\mathbf{\Lambda}_s^p$ when proper size of the master is chosen. In that case, retaining only the first item of the Taylor expansion, Eq. (22) is approximated as

$$\begin{bmatrix} \mathbf{\Lambda}_m^p - \overline{\lambda}\mathbf{I} & -\mathbf{\Gamma}_m \\ -\mathbf{\Gamma}_m^{\mathrm{T}} & -\mathbf{\Gamma}_s^{\mathrm{T}}(\mathbf{\Lambda}_s^p)^{-1}\mathbf{\Gamma}_s \end{bmatrix} \begin{Bmatrix} \mathbf{z}_m \\ \tau \end{Bmatrix} = \begin{Bmatrix} \mathbf{0} \\ \mathbf{0} \end{Bmatrix} \tag{24}$$

Resolving τ from the second equation of Eq. (24) and substituting it into the first equation, one can obtain that

$$[\mathbf{\Lambda}_m^p + \mathbf{\Gamma}_m(\mathbf{\Gamma}_s^{\mathrm{T}}(\mathbf{\Lambda}_s^p)^{-1}\mathbf{\Gamma}_s)^{-1}\mathbf{\Gamma}_m^{\mathrm{T}}]\mathbf{z}_m = \overline{\lambda}\mathbf{z}_m \tag{25}$$

then the final standard form of eigen-equation can be expressed as

$$\mathbf{\Psi}\mathbf{z}_m = \overline{\lambda}\mathbf{z}_m \tag{26}$$

where $\mathbf{\Psi} = \mathbf{\Lambda}_m^p + \mathbf{\Gamma}_m(\mathbf{\Gamma}_s^{\mathrm{T}}(\mathbf{\Lambda}_s^p)^{-1}\mathbf{\Gamma}_s)^{-1}\mathbf{\Gamma}_m^{\mathrm{T}}$, $\mathbf{\Gamma}(\mathbf{\Lambda}_s^p)^{-1}\mathbf{\Gamma}_s = \mathbf{C}\mathbf{\Phi}_s^p(\mathbf{\Lambda}_s^p)^{-1}[\mathbf{\Phi}_s^p]^{\mathrm{T}}\mathbf{C}^{\mathrm{T}}$.

$\mathbf{\Phi}_s^p(\mathbf{\Lambda}_s^p)^{-1}[\mathbf{\Phi}_s^p]^{\mathrm{T}}$ is regarded as the *first-order residual flexibility*. The detailed transformation concerning the first-order residual flexibility is given in Appendix B. The first-order residual flexibility of the jth substructure is

$$\mathbf{\Phi}_s^{(j)}(\mathbf{\Lambda}_s^{(j)})^{-1}[\mathbf{\Phi}_s^{(j)}]^{\mathrm{T}} = \mathbf{K}^{-1} - \mathbf{\Phi}_m^{(j)}(\mathbf{\Lambda}_m^{(j)})^{-1}[\mathbf{\Phi}_m^{(j)}]^{\mathrm{T}} \tag{27}$$

For the primitive system, the first-order residual flexibility is obtained as

$$\begin{aligned}
&\mathbf{\Phi}_s^p(\mathbf{\Lambda}_s^p)^{-1}[\mathbf{\Phi}_s^p]^{\mathrm{T}} \\
&= \begin{bmatrix} \mathbf{\Phi}_s^{(1)} & \mathbf{0} & \cdots & \mathbf{0} \\ \mathbf{0} & \mathbf{\Phi}_s^{(2)} & \cdots & \mathbf{0} \\ \vdots & \vdots & \ddots & \vdots \\ \mathbf{0} & \mathbf{0} & \cdots & \mathbf{\Phi}_s^{(NS)} \end{bmatrix} \begin{bmatrix} (\mathbf{\Lambda}_s^{(1)})^{-1} & \mathbf{0} & \cdots & \mathbf{0} \\ \mathbf{0} & (\mathbf{\Lambda}_s^{(2)})^{-1} & \cdots & \mathbf{0} \\ \vdots & \vdots & \ddots & \vdots \\ \mathbf{0} & \mathbf{0} & \cdots & (\mathbf{\Lambda}_s^{(NS)})^{-1} \end{bmatrix} \begin{bmatrix} [\mathbf{\Phi}_s^{(1)}]^{\mathrm{T}} & \mathbf{0} & \cdots & \mathbf{0} \\ \mathbf{0} & [\mathbf{\Phi}_s^{(2)}]^{\mathrm{T}} & \cdots & \mathbf{0} \\ \vdots & \vdots & \ddots & \vdots \\ \mathbf{0} & \mathbf{0} & \cdots & [\mathbf{\Phi}_s^{(NS)}]^{\mathrm{T}} \end{bmatrix} \\
&= \begin{bmatrix} \mathbf{\Phi}_s^{(1)}(\mathbf{\Lambda}_s^{(1)})^{-1}\left[\mathbf{\Phi}_s^{(1)}\right]^{\mathrm{T}} & \mathbf{0} & \cdots & \mathbf{0} \\ \mathbf{0} & \mathbf{\Phi}_s^{(2)}(\mathbf{\Lambda}_s^{(2)})^{-1}[\mathbf{\Phi}_s^{(2)}]^{\mathrm{T}} & \cdots & \mathbf{0} \\ \vdots & \vdots & \ddots & \vdots \\ \mathbf{0} & \mathbf{0} & \cdots & \mathbf{\Phi}_s^{(NS)}(\mathbf{\Lambda}_s^{(NS)})^{-1}[\mathbf{\Phi}_s^{(NS)}]^{\mathrm{T}} \end{bmatrix} \\
&= \begin{bmatrix} (\mathbf{K}^{(1)})^{-1} - \mathbf{\Phi}_m^{(1)}(\mathbf{\Lambda}_m^{(1)})^{-1}[\mathbf{\Phi}_m^{(1)}]^{\mathrm{T}} & \mathbf{0} & \cdots & \mathbf{0} \\ \mathbf{0} & (\mathbf{K}^{(2)})^{-1} - \mathbf{\Phi}_m^{(2)}\left(\mathbf{\Lambda}_m^{(2)}\right)^{-1}[\mathbf{\Phi}_m^{(2)}]^{\mathrm{T}} & \cdots & \mathbf{0} \\ \vdots & \vdots & \ddots & \vdots \\ \mathbf{0} & \mathbf{0} & \cdots & (\mathbf{K}^{(NS)})^{-1} - \mathbf{\Phi}_m^{(NS)}(\mathbf{\Lambda}_m^{(NS)})^{-1}[\mathbf{\Phi}_m^{(NS)}]^{\mathrm{T}} \end{bmatrix}
\end{aligned} \tag{28}$$

Therefore, the first-order residual flexibility of the primitive form can be regarded as the diagonal assembly of the substructures' first-order residual flexibility as

$$\mathbf{\Phi}_s^p(\mathbf{\Lambda}_s^p)^{-1}[\mathbf{\Phi}_s^p]^{\mathrm{T}} = \mathrm{Diag}[((\mathbf{K}^{(1)})^{-1} - \mathbf{\Phi}_m^{(1)}(\mathbf{\Lambda}_m^{(1)})^{-1}[\mathbf{\Phi}_m^{(1)}]^{\mathrm{T}}), \ldots, ((\mathbf{K}^{(NS)})^{-1} - \mathbf{\Phi}_m^{(NS)}(\mathbf{\Lambda}_m^{(NS)})^{-1}[\mathbf{\Phi}_m^{(NS)}]^{\mathrm{T}})] \tag{29}$$

Subsequently, the eigen-equation (Eq. (26)) can be evaluated with standard Subspace Iteration or Lanczos method [26]. The eigenvectors $\mathbf{z}$ of this equation are based on the modal coordinates. The expanded

eigenvectors of the global structure in the physical coordinates can be recovered by

$$\overline{\mathbf{\Phi}} = \mathbf{\Phi}_m^p \mathbf{z}_m \tag{30}$$

Finally, the eigenvectors of the global structure $\mathbf{\Phi}$ can be directly obtained after discarding the identical values at the tearing points in $\overline{\mathbf{\Phi}}$.

In this section, the higher modes of the substructures are compensated by the first-order residual flexibility, which is entitled as First-order residual flexibility-based substructuring (FRFS) method. The matrix $\mathbf{\Psi}$ for eigensolutions is reduced to the size of $m^p \times m^p$, which is much less than the original one ($NP \times NP$). In the FRFS method, only the first item of Taylor expansion is retained. Theoretically, this simplification is accurate only at zero frequency. The approximation is satisfied when the interested eigenvalues $\overline{\lambda}$ are far less than the minimum value of $\mathbf{\Lambda}_s^p$. If the interested eigenvalues become large, the results may be not accurate enough. Therefore, if a higher calculation precision is required, the second item of Taylor expansion (Eq. (23)) should be retained.

4. Second-order residual flexibility based modal truncation

If the first two items of the Taylor expansion in Eq. (23) are retained, Eq. (22) becomes

$$\begin{bmatrix} \mathbf{\Lambda}_m^p - \overline{\lambda}\mathbf{I} & -\mathbf{\Gamma}_m \\ -\mathbf{\Gamma}_m^{\mathrm{T}} & -(\mathbf{\Gamma}_s^T(\mathbf{\Lambda}_s^p)^{-1}\mathbf{\Gamma}_s + \overline{\lambda}\mathbf{\Gamma}_s^{\mathrm{T}}(\mathbf{\Lambda}_s^p)^{-2}\mathbf{\Gamma}_s) \end{bmatrix} \begin{Bmatrix} \mathbf{z}_m \\ \tau \end{Bmatrix} = \begin{Bmatrix} \mathbf{0} \\ \mathbf{0} \end{Bmatrix} \tag{31}$$

After arranging Eq. (31), the standard form of eigen-equation can be expressed as

$$\begin{bmatrix} \mathbf{\Lambda}_m^p & -\mathbf{\Gamma}_m \\ -\mathbf{\Gamma}_m^{\mathrm{T}} & -\mathbf{\Gamma}_s^{\mathrm{T}}(\mathbf{\Lambda}_s^p)^{-1}\mathbf{\Gamma}_s \end{bmatrix} \begin{Bmatrix} \mathbf{z}_m \\ \tau \end{Bmatrix} = \overline{\lambda} \begin{bmatrix} \mathbf{I} & \mathbf{0} \\ \mathbf{0} & \mathbf{\Gamma}_s^{\mathrm{T}}(\mathbf{\Lambda}_s^p)^{-2}\mathbf{\Gamma}_s \end{bmatrix} \begin{Bmatrix} \mathbf{z}_m \\ \tau \end{Bmatrix} \tag{32}$$

In Eq. (32),

$$\begin{cases} \mathbf{\Gamma}_s^{\mathrm{T}}(\mathbf{\Lambda}_s^p)^{-1}\mathbf{\Gamma}_s = \mathbf{C}\mathbf{\Phi}_s^p(\mathbf{\Lambda}_s^p)^{-1}[\mathbf{\Phi}_s^p]^{\mathrm{T}}\mathbf{C}^{\mathrm{T}} \\ \mathbf{\Gamma}_s^{\mathrm{T}}(\mathbf{\Lambda}_s^p)^{-2}\mathbf{\Gamma}_s = \mathbf{C}\mathbf{\Phi}_s^p(\mathbf{\Lambda}_s^p)^{-2}[\mathbf{\Phi}_s^p]^{\mathrm{T}}\mathbf{C}^{\mathrm{T}} \end{cases} \tag{33}$$

$\mathbf{\Phi}_s^p(\mathbf{\Lambda}_s^p)^{-2}[\mathbf{\Phi}]^{\mathrm{T}}$ is referred to as the *second-order residual flexibility*. Formation of the second-order residual flexibility can be found in Appendix B. With the same procedure described in previous section, the primitive form of the second-order residual flexibility can also be obtained by the diagonal assembling of the substructures' second-order residual flexibility as

$$\begin{aligned} \mathbf{\Phi}_s^p(\mathbf{\Lambda}_s^p)^{-2}[\mathbf{\Phi}_s^p]^{\mathrm{T}} = \mathrm{Diag}[&((\mathbf{K}^{(1)})^{-1}\mathbf{M}(\mathbf{K}^{(1)})^{-1} - \mathbf{\Phi}_m^{(1)}(\mathbf{\Lambda}_m^{(1)})^{-2}[\mathbf{\Phi}_m^{(1)}]^{\mathrm{T}}), \ldots, ((\mathbf{K}^{(NS)})^{-1}\mathbf{M}(\mathbf{K}^{(NS)})^{-1} \\ &- \mathbf{\Phi}_m^{(NS)}(\mathbf{\Lambda}_m^{(NS)})^{-2}[\mathbf{\Phi}_m^{(NS)}]^{\mathrm{T}})] \end{aligned} \tag{34}$$

With both the first- and second-order flexibility in Eqs. (29) and (34), the subsequent procedure of obtaining the eigensolutions of the global structure is similar with that of the FRFS method.

As compared with the FRFS procedure introduced previously, this second-order residual flexibility-based substructuring (SRFS) method will achieve much more accurate results since it includes the second item in the Taylor expansion. However, this high precision is achieved at the cost of computation load in terms of two aspects: (i) the SRFS method has to spend some additional CPU effort to calculate the second-order residual flexibility $\mathbf{\Phi}_s^p(\mathbf{\Lambda}_s^p)^{-2}[\mathbf{\Phi}_s^p]^{\mathrm{T}}$; and (ii) the size of the eigen-equation in the SRFS method (Eq. (32)), which contains the 'misfit' displacement at tearing points, is larger than that of the FRFS method.

5. Error quantification

In the FRFS method, the approximation is introduced by replacing $(\mathbf{\Lambda}_s^p - \overline{\lambda}\mathbf{I})^{-1}$ with $(\mathbf{\Lambda}_s^p)^{-1}$. Consequently, the error introduced by this approximation is

$$\text{Error} = (\mathbf{\Lambda}_s^p - \overline{\lambda}\mathbf{I})^{-1} - (\mathbf{\Lambda}_s^p)^{-1} = \begin{bmatrix} \dfrac{1}{(\mathbf{\Lambda}_s^p)_1 - \overline{\lambda}} - \dfrac{1}{(\mathbf{\Lambda}_s^p)_1} & & \\ & \ddots & \\ & & \dfrac{1}{(\mathbf{\Lambda}_s^p)_{s^\pi} - \overline{\lambda}} - \dfrac{1}{(\mathbf{\Lambda}_s^p)_{s^\pi}} \end{bmatrix}$$

$$= \begin{bmatrix} \dfrac{\overline{\lambda}}{((\mathbf{\Lambda}_s^p)_1 - \overline{\lambda})(\mathbf{\Lambda}_s^p)_1} & & \\ & \ddots & \\ & & \dfrac{\overline{\lambda}}{((\mathbf{\Lambda}_s^p)_{s^p} - \overline{\lambda})(\mathbf{\Lambda}_s^p)_{s^p}} \end{bmatrix} = \text{Diag}\left(\frac{\overline{\lambda}}{((\mathbf{\Lambda}_s^p)_i - \overline{\lambda})(\mathbf{\Lambda}_s^p)_i}\right) \tag{35}$$

$$\text{Relative error} = \text{Diag}\left(\frac{\frac{\overline{\lambda}}{((\mathbf{\Lambda}_s^p)_i - \overline{\lambda})(\mathbf{\Lambda}_s^p)_i}}{\frac{1}{(\mathbf{\Lambda}_s^p)_i - \overline{\lambda}}}\right) = \text{Diag}\left(\frac{\overline{\lambda}}{(\mathbf{\Lambda}_s^p)_i}\right) \quad (i = 1, 2, \ldots, s^p) \tag{36}$$

Therefore, the largest relative error $= \overline{\lambda}/\min(\mathbf{\Lambda}_s^p)$.

Similarly, in the SRFS method, the error introduced by Taylor expansion is

$$Error = (\mathbf{\Lambda}_s^p - \overline{\lambda}\mathbf{I})^{-1} - (\mathbf{\Lambda}_s^p)^{-1} - \overline{\lambda}(\mathbf{\Lambda}_s^p)^{-2} = \text{Diag}\left(\frac{1}{(\mathbf{\Lambda}_s^p)_i - \overline{\lambda}} - \frac{1}{(\mathbf{\Lambda}_s^p)_i} - \frac{\overline{\lambda}}{(\mathbf{\Lambda}_s^p)_i^2}\right)$$

$$= \text{Diag}\left(\frac{(\mathbf{\Lambda}_s^p)_i^2 - ((\mathbf{\Lambda}_s^p)_i - \overline{\lambda})(\mathbf{\Lambda}_s^p)_i - \overline{\lambda}((\mathbf{\Lambda}_s^p)_i - \overline{\lambda})}{((\mathbf{\Lambda}_s^p)_i - \overline{\lambda})(\mathbf{\Lambda}_s^p)_i^2}\right) = \text{Diag}\left(\frac{\overline{\lambda}^2}{((\mathbf{\Lambda}_s^p)_i - \overline{\lambda}\mathbf{I})(\mathbf{\Lambda}_s^p)_i^2}\right) \tag{37}$$

$$\text{Relative error} = \text{Diag}\left(\frac{\frac{\overline{\lambda}^2}{((\mathbf{\Lambda}_s^p)_i - \overline{\lambda})(\mathbf{\Lambda}_s^p)_i^2}}{\frac{1}{(\mathbf{\Lambda}_s^p)_i - \overline{\lambda}}}\right) = \text{Diag}\left(\left(\frac{\overline{\lambda}}{(\mathbf{\Lambda}_s^p)_i}\right)^2\right) \quad (i = 1, 2, \ldots, s^p) \tag{38}$$

The largest relative error $= (\overline{\lambda}/\min(\mathbf{\Lambda}_s^p))^2$.

The relative error in both the FRFS method and the SRFS method is dependent on $\overline{\lambda}/\min(\mathbf{\Lambda}_s^p)$. This demonstrates that, if the required eigenvalues $\overline{\lambda}$ are far less than the minimum value of $\mathbf{\Lambda}_s^p$, the introduced error will be insignificant. The minimum value of $\mathbf{\Lambda}_s^p$ will control the accuracy of the method. Since general eigensolvers can compute some lowest eigensolutions, one should determine how many master modes need to be calculated in each substructure. This will be described in later examples.

6. Example 1: a frame structure

The first example presented here serves to illustrate the entire procedure of the proposed substructuring method in details.

The global frame is shown in Fig. 1. The material constants are chosen as: bending rigidity $(EI) = 170 \times 10^6\,\text{N m}^2$, axial rigidity $(EA) = 2500 \times 10^6\,\text{N}$, mass per unit length $(\rho A) = 110\,\text{kg/m}$, and Poisson's ratio $= 0.3$. The frame is discretized into 160 two-dimensional beam elements each 2.5 m long, which results in 140 nodes and 408 dofs ($N = 408$). The frame is disassembled into three substructures ($NS = 3$) when it is torn at eight nodes as shown in Fig. 2. After division, there are 51, 55, 42 nodes in the three substructures with the dofs of

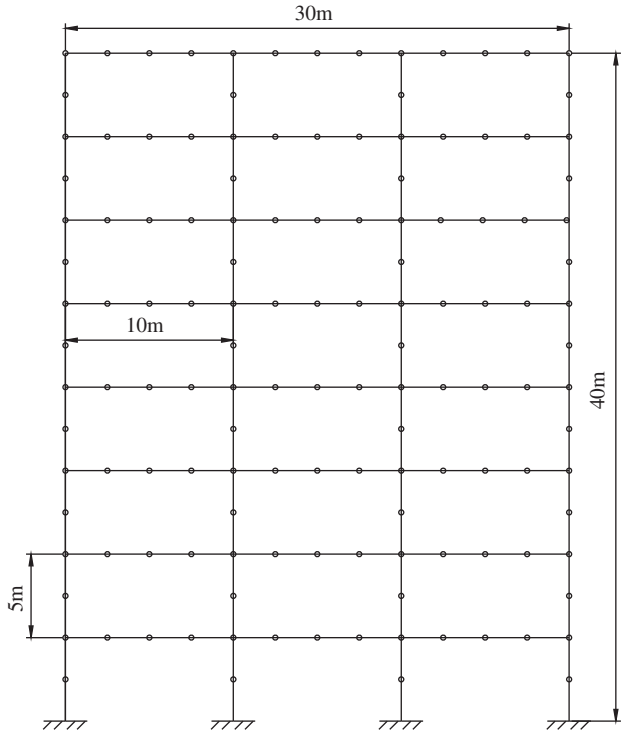

Fig. 1. The original global frame.

$n_1 = 153$, $n_2 = 165$, $n_3 = 114$, respectively. The eight tearing nodes introduce 48 tearing dofs (each node has 3 dofs) with 24 identical/repeated ones. Therefore, the primitive form of the assembled substructures have $NP = 432$ dofs in total and $NT = 24$ displacement constraints.

For comparison, the frame will be analyzed with four approaches to extract the first 20 eigensolutions of the global structure.

In the first approach, the frame is analyzed by the original Kron's substructuring method [18], in which the whole eigensolutions of each substructure are calculated to assemble the primitive matrices. The primitive matrices have the size of 432×432 and are solved with the standard Lanczos eigensolver. Because the contribution of the complete modes in each substructure is considered and there is no approximation during the whole process, the obtained eigensolutions can be regarded as accurate.

In the second approach, the first 50 modes of each substructure are calculated, while the residual high modes are discarded directly. Other than the proposed method, the residual high modes here are discarded without any compensation. Similar to the previous process, the eigen-equation can be obtained but with the size of 150×150.

Thirdly, the frame is analyzed by the proposed method with the FRFS scheme. The first 50 modes in each substructure are chosen as 'master', while the higher modes are compensated by the first-order residual flexibility. The procedure consists of the following steps:

(1) Divide the global structure into three substructures. Each substructure is regarded an independent structure, and the nodes and elements are labeled individually.
(2) Obtain the first 50 eigensolutions of the three substructures, and calculate the first-order residual flexibility of each substructure. For the substructures 1 and 2, a small shift '1' is introduced because the two substructures become free-free and include zero frequencies.
(3) Assemble the primitive form of the master eigensolutions $\mathbf{\Lambda}_m^p$ and $\mathbf{\Phi}_m^p$ with the master modes of the three substructures. $\mathbf{\Lambda}_m^p$and $\mathbf{\Phi}_m^p$ are the size of 150×150 and 150×432, respectively.

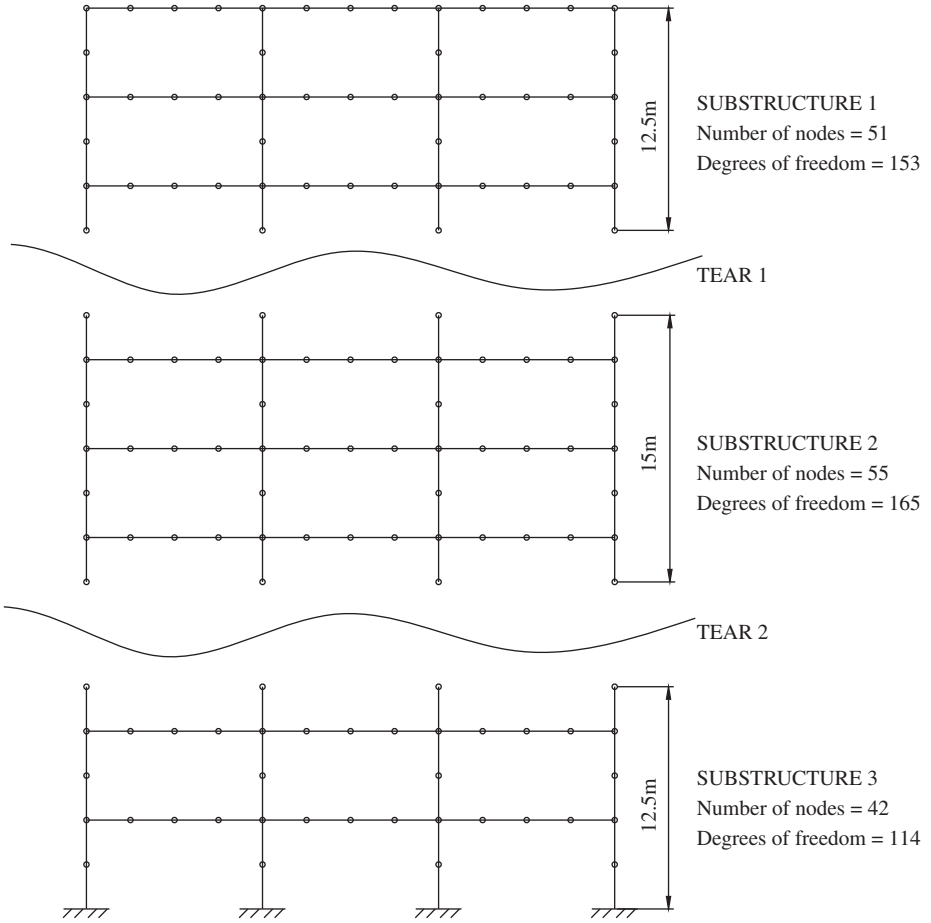

Fig. 2. The primitive system with three substructures.

(4) Process the connection matrix **C**. There are eight tearing points and each has 3 dofs, which introduce the connection matrix of order 24×432.
(5) Form the matrix $\mathbf{\Psi}$ of order 150×150 in Eq. (26) according to the procedure described in Section 3, and solve the eigen-equation with standard Lanczos method.
(6) Recover the eigenvectors of the global structure by discarding the identical coordinates from the expanded eigenvectors of the global structure.

Finally, the frame is investigated with the SRFS method. Likewise, the first 50 modes in each substructure are chosen as master modes. The process is similar to the FRFS method except the final step in forming the eigen-equation. In this step, the eigen-equation (Eq. (32)) contains the 'misfit' displacement τ, and has the size of 174×174. The eigensolutions of the global structure can then be obtained from this eigen-equation.

The first 20 frequencies of the global structure are obtained from the above-mentioned four approaches and listed in Table 1 for comparison. In this table, 'Lanczos' represents the results obtained from the traditional Lanczos method without substructuring; 'Original' refers to the original Kron's substructuring method, which includes all eigensolutions of each substructure; 'Original-Partial' represents the substructuring method adopting partial modes, in which only the first 50 modes are retained while the residual higher modes are discarded directly; 'FRFS' indicates the proposed FRFS method, and 'SRFS' indicates the proposed SRFS method. The second line of Table 1 gives the required CPU time (in second) to obtain the first 20 modes of the global structure with the corresponding methods on a PC with 1.86 GHz Intel Core 2 Duo processor and 2 GB memory.

Table 1
The frequencies and modal shapes of the global structure obtained with different techniques.

	Lanczos	Original	Original–Partial		FRFS				SRFS			
CPU time (s)	0.1703	0.5640	0.1671		0.1978				0.2413			
Mode index	Frequency (Hz)	Frequency (Hz)	Frequency (Hz)	Relative error (%)	Frequency (Hz)	Relative error (%)	Mode shape error		Frequency (Hz)	Relative error (%)	Mode shape error	
							(1-MAC) (%)	Difference Norm (%)			(1-MAC) (%)	Difference Norm (%)
1	1.7837	1.7837	1.7898	0.341	1.7837	0.000	0.000	0.000	1.7837	0.000	0.000	0.000
2	5.5197	5.5197	5.5495	0.539	5.5197	0.000	0.000	0.000	5.5197	0.000	0.000	0.000
3	9.7392	9.7392	9.7959	0.582	9.7393	0.001	0.003	0.006	9.7392	0.000	0.003	0.005
4	14.4631	14.4631	14.5231	0.415	14.4633	0.001	0.002	0.003	14.4631	0.000	0.002	0.002
5	16.5938	16.5938	18.8166	13.396	16.5995	0.034	0.081	0.000	16.5938	0.000	0.081	0.000
6	18.6944	18.6944	19.8156	5.997	18.7055	0.060	0.130	0.018	18.6946	0.001	0.130	0.021
7	19.7277	19.7277	21.1509	7.214	19.7283	0.003	0.006	0.018	19.7277	0.000	0.006	0.018
8	22.3255	22.3255	25.0778	12.328	22.3502	0.111	0.236	0.029	22.3261	0.002	0.236	0.028
9	24.9127	24.9127	25.4569	2.184	24.9227	0.040	0.099	0.085	24.9128	0.001	0.094	0.040
10	25.4016	25.4016	27.0610	6.533	25.4063	0.018	0.058	0.019	25.4017	0.000	0.044	0.011
11	26.6811	26.6811	27.6134	3.494	26.6832	0.008	0.016	0.062	26.6812	0.000	0.015	0.062
12	28.2301	28.2301	28.5257	1.047	28.2349	0.017	0.043	0.109	28.2302	0.000	0.043	0.108
13	29.3925	29.3925	29.8720	1.632	29.4019	0.032	0.069	0.141	29.3928	0.001	0.068	0.139
14	30.1068	30.1068	30.1980	0.303	30.1080	0.004	0.009	0.020	30.1068	0.000	0.009	0.019
15	30.7279	30.7279	30.8539	0.410	30.7298	0.006	0.007	0.047	30.7280	0.000	0.007	0.046
16	30.8943	30.8943	31.0906	0.635	30.8981	0.012	0.023	0.047	30.8944	0.000	0.023	0.039
17	31.9437	31.9437	32.0649	0.379	31.9460	0.007	0.019	0.067	31.9438	0.000	0.018	0.066
18	32.1127	32.1127	32.3354	0.693	32.1172	0.014	0.034	0.039	32.1129	0.000	0.033	0.033
19	32.8386	32.8386	33.0881	0.760	32.8437	0.015	0.037	0.085	32.8388	0.001	0.034	0.084
20	32.8395	32.8395	33.1796	1.036	32.8476	0.025	0.051	0.048	32.8398	0.001	0.048	0.041

Other than frequency, mode shape (eigenvector) is another significant data during model updating and damage identification. There are two means utilized to check the eigenvector's accuracy of this substructuring method. Firstly, the popularly used modal assurance criterion (MAC) [27] gives the similarity of two sets of mode shapes as

$$\mathrm{MAC}(\{\phi_i\},\{\tilde{\phi}_i\}) = \frac{|\{\phi_i\}^{\mathrm{T}}\{\tilde{\phi}_i\}|^2}{(\{\phi_i\}^{\mathrm{T}}\{\phi_i\})(\{\tilde{\phi}_i\}^{\mathrm{T}}\{\tilde{\phi}_i\})} \tag{39}$$

In addition, employing the Frobenius norm, the *difference norm* is applied to indicate the relative error of mode shapes as

$$\text{Difference norm} = \frac{norm(\{\phi_i\} - \{\tilde{\phi}_i\})}{\mathrm{norm}(\{\phi_i\})} \tag{40}$$

in which, $\{\phi_i\}$ is the ith accurate eigenvector obtained from Lanczos method, $\{\tilde{\phi}_i\}$ represents the ith eigenvector achieved by the proposed substructuring method. The eigenvectors' errors checked by the above two methods are listed in Table 1.

From Table 1, one can find that:

(1) As compared with the traditional Lanczos method, the original Kron's substructuring method is very time-consuming.
(2) Utilization of the partial modes introduces a large error. Since the substructures are connected based on the principle of virtual work, discarding the energy contribution of the higher modes definitely results in unexpected error.
(3) With the proposed method, in which the higher modes are taking into consideration via residual flexibility, the accuracy of eigenvalues is improved significantly. For example, the relative errors of the first 20 frequencies are less than 0.1% with the FRFS method, and less than 0.002% with the SRFS method. The

Table 2
The size of eigen-equation with various methods.

	Lanczos	Original Kron's method	FRFS	SRFS
Sub 1		153×153	50×50	50×50
Sub 2		165×165	50×50	50×50
Sub 3		142×142	50×50	50×50
Global structure	408×408	432×432	150×150	174×174

accuracy achieved is sufficient for usual engineering applications. As compared with the traditional Kron's substructuring method, the proposed method reduces the computation loads significantly.

(4) The SRFS method can achieve a higher precision than the FRFS method, but it costs more computation effort and larger memory.

(5) The proposed method not only can convincingly achieve a high precision eigenvalue but also a good eigenvector result.

(6) The proposed substructuring method takes up a little longer time than the Lanczos method without substructuring. This is because the analyses of each substructure costs a lot of computation effort, especially calculating the residual flexibility of each substructure. However, the substructuring methods are promising in the model updating and damage identification applications. With the proposed method, the repeated calculation of eigensolutions and sensitivity matrix are only required for the substructures of interest. In addition, the eigen-equation size of the proposed method is much less than that of the Lanczos method and the original Kron's substructuring method, as listed in Table 2. This is an attractive merit for model updating process, which will be studied in the near future.

This simple example indicates that the proposed modal truncation in the substructuring method can reduce computation load significantly while satisfying a high accuracy. Although the accuracy of the FRFS method is not as good as that of the SRFS method, it can satisfy most of engineering applications and cost much less computation resource. Therefore, the FRFS method might be preferable in practical engineering. In the second example, only the FRFS method will be utilized.

7. Example 2: a practical bridge

To illustrate the efficiency of the proposed method in obtaining the eigensolutions of relatively large structures, a practical bridge [28] is employed here. The FE model of this bridge has 907 elements, 947 nodes each has six dofs, and 5420 dofs in total as shown in Fig. 3. The global structure is divided into five substructures. The tearing points are located at 10, 20, 30 and 40 m along the longitudinal direction. The detailed information of the five substructures is listed in Table 3.

In this example, only the FRFS method is utilized, and the first 40 modes in each substructure are chosen as master modes. The first 20 eigensolutions of the global structure are calculated and the frequencies are listed in Table 4, together with the relative errors of the frequencies compared with the exact results using Lanczos method.

To investigate the effect of the number of the master modes, 60, 80 and 90 modes in each substructure are chosen as 'master'. The results and corresponding errors are listed in Table 4. Obviously, the accuracy of frequencies is improved when more master modes are included in each substructure.

The required number of master modes in each substructure depends on the accuracy requirement. Based on the error analysis previously described, one should make the minimum value of $\mathbf{\Lambda}_s^p$ as large as possible. Sturm's Sequence check [25] can be employed to determine the number of eigensolutions which are smaller than a specified value. Nevertheless, when the substructures are similarly divided, one can choose the same number of master modes in each substructure. From the two examples in this paper, when choosing 40–60 master modes in each substructure, the relative errors of the first 20 frequencies are less than 0.1% for the FRFS method. It is usually sufficient for model updating and damage identification applications. In this

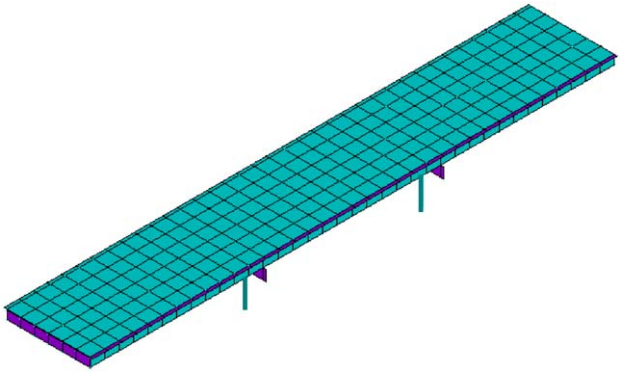

Fig. 3. The finite element model of the Balla Balla River Bridge.

Table 3
Information of the substructures.

Index of substructures	Sub 1	Sub 2	Sub 3	Sub 4	Sub 5
Geometric range (m)[a]	0–10	10–20	20–30	30–40	40–54
No. element	187	182	132	182	224
No. node	205	212	161	212	251
No. dofs	1095	1260	966	1260	1371
No. tearing dofs	138	138	138	138	

[a]In longitudinal direction.

Table 4
The comparison of different master modes quantity.

	Exact	Original	40 Master modes		60 Master modes		80 Master modes		90 Master modes	
CPU time (s)	8.0253	238.8509	10.3725		10.9643		12.0360		13.0231	
Mode index	Frequency (Hz)	Frequency (Hz)	Frequency (Hz)	Relative error (%)	Frequency (Hz)	Relative error (%)	Frequency (Hz)	Relative error (%)	Frequency (Hz)	Relative error (%)
1	5.8232	5.8232	5.8288	0.097	5.8281	0.084	5.8269	0.064	5.8269	0.063
2	5.9998	5.9998	6.0028	0.051	6.0028	0.051	6.0028	0.051	6.0028	0.051
3	6.0007	6.0007	6.0038	0.052	6.0038	0.051	6.0037	0.051	6.0037	0.051
4	6.2635	6.2635	6.2691	0.089	6.2677	0.066	6.2670	0.055	6.2669	0.053
5	6.8621	6.8621	6.8656	0.051	6.8655	0.051	6.8655	0.051	6.8655	0.051
6	6.8987	6.8987	6.9023	0.052	6.9023	0.052	6.9022	0.051	6.9022	0.051
7	6.9975	6.9975	7.0034	0.084	7.0022	0.067	7.0012	0.053	7.0012	0.052
8	7.7391	7.7391	7.7465	0.095	7.7449	0.075	7.7434	0.056	7.7432	0.053
9	8.6063	8.6063	8.6142	0.092	8.6128	0.075	8.6110	0.054	8.6109	0.053
10	8.7145	8.7145	8.7205	0.069	8.7197	0.059	8.7191	0.053	8.7191	0.052
11	9.4460	9.4460	9.4535	0.079	9.4525	0.068	9.4510	0.053	9.4510	0.053
12	10.9814	10.9814	10.9870	0.051	10.9870	0.051	10.9870	0.051	10.9870	0.051
13	10.9816	10.9816	10.9872	0.051	10.9872	0.051	10.9872	0.051	10.9872	0.051
14	12.1302	12.1302	12.1511	0.172	12.1417	0.094	12.1387	0.070	12.1375	0.059
15	13.0048	13.0048	13.0227	0.137	13.0167	0.091	13.0126	0.060	13.0122	0.057
16	13.2693	13.2693	13.2868	0.132	13.2810	0.088	13.2771	0.059	13.2767	0.056
17	14.9312	14.9312	14.9431	0.080	14.9421	0.073	14.9405	0.062	14.9399	0.058
18	15.8194	15.8194	15.8880	0.434	15.8610	0.263	15.8347	0.097	15.8337	0.090
19	16.9266	16.9266	16.9515	0.147	16.9463	0.116	16.9380	0.067	16.9370	0.062
20	17.5480	17.5480	17.6043	0.321	17.5646	0.095	17.5609	0.074	17.5602	0.070

Table 5
The size of eigen-equation with various methods.

	Lanczos	Kron's original method	FRFS
Sub 1		1095×1095	60×60
Sub 2		1260×1260	60×60
Sub 3		966×966	60×60
Sub 4		1260×1260	60×60
Sub 5		1371×1371	60×60
Global structure	5420×5420	5952×5952	300×300

Table 6
The matrix size and computation time with different division formation.

No. substructures	3	5	8	11
Scheme 1				
No. master modes in each substrucutre	80	80	80	80
Eigen-equation size of the global structure	240	400	640	880
CPU time (s)	20.8	12.8	16.7	26.1
Scheme 2				
No. master modes in each substrucutre	133	80	50	37
Eigen-equation size of the global structure	399	400	400	407
CPU time (s)	24.9	12.8	13.4	22.7

example, when 60 master modes are chosen in each substructure, the eigen-equation size of the global structure can be heavily reduced with the proposed FRFS method as listed in Table 5.

Certainly, not only the master modes selection but also the division formation of the substructures will influence the accuracy and efficiency. For a determined global structure, there are various division formations of the substructures. From a practical point of view, cutting a building through columns' joints is better than through the slabs, and cutting a bridge avoiding the piers is better than across the piers, in order to reduce the interface joints. This can reduce the size of the transformation matrix $\mathbf{C}$.

To investigate the influence of the substructures' division formation, the bridge is approximately averaged into 3, 5, 8, 11 substructures, respectively, along the longitudinal direction. For the different division formations, the selection criterion of the master modes is considered in the following two schemes.

In the first scheme, the first 80 modes in each substructure are chosen as master modes. The master modes in each substructure and the eigen-equation size of the global structure are listed in Table 6, together with the corresponding CPU time spent on calculating the first 40 eigensolutions of the global structure. The relative errors of frequencies are compared in Fig. 4.

It can be found that, except dividing the global structure into three substructures, other three division formations achieve similar accuracy, although the division formation with more substructures can achieve a slightly better precision.

The division formations of three and eleven substructures cost more computation time than that of five and eight. This is because too few substructures cause each substructure has a large amount of elements and nodes. Correspondently, calculation of the eigensolutions and the residual flexibility of each substructure will cost more CPU resource. On the other hand, the global structure is divided into more substructures. Although each substructure has smaller size, one has to cope with more substructures. In addition, the final eigen-equation of the global structure has a larger size. From the comparison of these four division formations, it can be concluded that dividing the global structure into much excessive substructures or too few substructures are both unpreferable. In this case study, dividing the global structure into five substructures cannot only reach the high precision but also save computation resource.

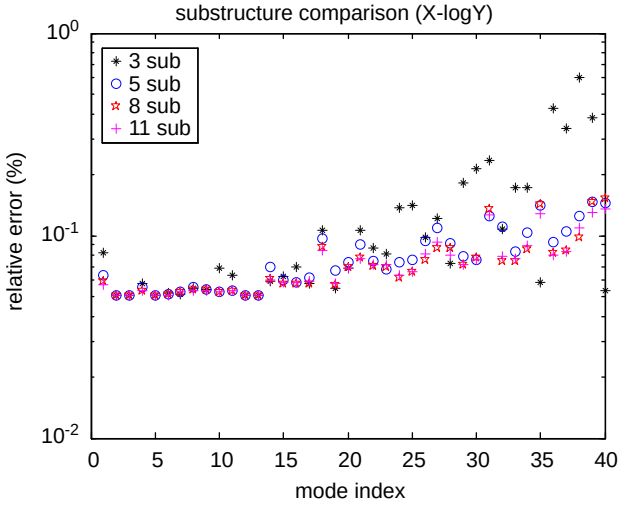

Fig. 4. The relative errors of frequencies with various substructure division formations (scheme 1).

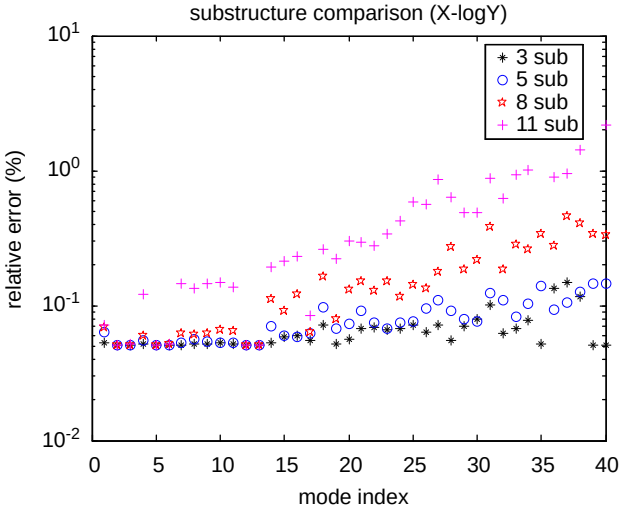

Fig. 5. The relative errors of frequencies with various substructure division formations (scheme 2).

In the second scheme, the total number of master modes is selected around 400, but each substructure has different number of master modes, as listed in Table 6. The CPU time cost in calculating the first 40 eigensolutions of the global structure with these four division formations are listed in Table 6, and the relative errors of frequencies are compared in Fig. 5.

Fig. 5 shows that, if the total number of the master modes among all substructures is determined, more substructures will result in lower precision. This is because more substructures imply less master modes in each substructure, and thus $\min(\mathbf{\Lambda}_s^p)$ is not big enough. In contrast, fewer substructures will achieve a higher precision, since it includes more master modes in each substructure. However, if the global structure is divided into too few substructures, it will cost much CPU time to calculate the eigensolutions and the residual flexibility matrix for the big substructures. Furthermore, when applying the substructuring method in model updating, the calculation of the sensitivity matrix in each substructure will be heavier, and the substructuring technology may lose its promising advantages. In practice, a few trials may be helpful before model updating and/or damage identification is employed.

8. Conclusions and discussions

A substructuring method has been presented in this paper to calculate some lowest eigensolutions of large-scale structures. A modal truncation approximation is proposed to reduce the computation load. With the compensation of the residual flexibility, only a few eigensolutions of the substructures are needed. A frame with hundreds of dofs and a bridge structure with thousands of dofs are used to illustrate the procedures of the proposed method. For super-large structures such as those with millions of dofs, traditional eigensolutions may be more difficult and time-consuming as even storage of entire system matrices is prohibited. The substructuring method can be a promising option, or combined with some other reduction techniques such as Ref. [5]. This merits further studies.

There are two strategies to improve the calculation precision, that is, selecting more master modes in the substructures or utilizing the SRFS method instead of the FRFS method. The utilization of the second-order residual flexibility can achieve much better results than that of the first-order residual flexibility, while increases the computation effort greatly. Furthermore, similar to the model reduction technique [6,25], the proposed substructuring method may be developed by combining an iterative model reduction scheme.

For a determined structure, dividing it into excessive or insufficient number of substructures are both undesirable. The division formations need to trade off the number of substructures and the number of master modes in each substructure.

The more significant merit of the proposed method lies in the applications to model updating and damage identification. In general, model updating and damage identification need to re-calculate the eigensolutions and sensitivity matrix of the entire structure when the parameters of some elements are changed. With the substructuring method, only particular substructures need to be re-analyzed, while other substructures can be untouched. This will be studied in the future.

Acknowledgment

The work described in this paper is supported by a grant from the Research Grants Council of the Hong Kong Special Administrative Region, China (Project no. PolyU 5321/08E).

Appendix A. Transformation matrix

This section aims to illustrate the procedure of the substructuring method and the associated symbols using a simple structure.

The global structure has two elements and three nodes (a, b, c) each has 3 dofs as Fig. A1(a). It is torn into two substructures at node b as Fig. A1(b).The node b at tearing point is expanded into node b_1 and node b_2 in the two substructures.

If $\{\overline{x}_1, \overline{x}_2, \overline{x}_3\}^{\mathrm{T}}$ is the displacement vector of node a in substructure 1, and $\{\overline{x}_4, \overline{x}_5, \overline{x}_6\}^{\mathrm{T}}$ is the displacement vector of node b_1 in substructure 1, the eigensolutions of the first substructure are written as

$$\mathbf{\Lambda}^{(1)} = \mathrm{Diag}[\lambda_1^{(1)}, \lambda_2^{(1)}, \lambda_3^{(1)}, \lambda_4^{(1)}, \lambda_5^{(1)}, \lambda_6^{(1)}], \quad \mathbf{\Phi}^{(1)} = \begin{bmatrix} \phi_{1,1}^{(1)} & \phi_{1,2}^{(1)} & \phi_{1,3}^{(1)} & \phi_{1,4}^{(1)} & \phi_{1,5}^{(1)} & \phi_{1,6}^{(1)} \\ \phi_{2,1}^{(1)} & \phi_{2,2}^{(1)} & \phi_{2,3}^{(1)} & \phi_{2,4}^{(1)} & \phi_{2,5}^{(1)} & \phi_{2,6}^{(1)} \\ \phi_{3,1}^{(1)} & \phi_{3,2}^{(1)} & \phi_{3,3}^{(1)} & \phi_{3,4}^{(1)} & \phi_{3,5}^{(1)} & \phi_{3,6}^{(1)} \\ \phi_{4,1}^{(1)} & \phi_{4,2}^{(1)} & \phi_{4,3}^{(1)} & \phi_{4,4}^{(1)} & \phi_{4,5}^{(1)} & \phi_{4,6}^{(1)} \\ \phi_{5,1}^{(1)} & \phi_{5,2}^{(1)} & \phi_{5,3}^{(1)} & \phi_{5,4}^{(1)} & \phi_{5,5}^{(1)} & \phi_{5,6}^{(1)} \\ \phi_{6,1}^{(1)} & \phi_{6,2}^{(1)} & \phi_{6,3}^{(1)} & \phi_{6,4}^{(1)} & \phi_{6,5}^{(1)} & \phi_{6,6}^{(1)} \end{bmatrix} \tag{A.1}$$

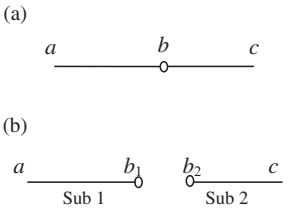

Fig. A1. Two element connected point: (a) the global structure and (b) the substructures.

Similarly, $\{\overline{x}_7, \overline{x}_8, \overline{x}_9\}^{\mathrm{T}}$ and $\{\overline{x}_{10}, \overline{x}_{11}, \overline{x}_{12}\}^{\mathrm{T}}$ is the displacement vectors of nodes b_2 and c in substructure 2, respectively. To be an independent structure, the eigensolutions of the second substructure are

$$\mathbf{\Lambda}^{(2)} = \mathrm{Diag}[\lambda_1^{(2)}, \ldots, \lambda_6^{(2)}], \quad \mathbf{\Phi}^{(2)} = \begin{bmatrix} \phi_{1,1}^{(2)} & \phi_{1,2}^{(2)} & \phi_{1,3}^{(2)} & \phi_{1,4}^{(2)} & \phi_{1,5}^{(2)} & \phi_{1,6}^{(2)} \\ \phi_{2,1}^{(2)} & \phi_{2,2}^{(2)} & \phi_{2,3}^{(2)} & \phi_{2,4}^{(2)} & \phi_{2,5}^{(2)} & \phi_{2,6}^{(2)} \\ \phi_{3,1}^{(2)} & \phi_{3,2}^{(2)} & \phi_{3,3}^{(2)} & \phi_{3,4}^{(2)} & \phi_{3,5}^{(2)} & \phi_{3,6}^{(2)} \\ \phi_{4,1}^{(2)} & \phi_{4,2}^{(2)} & \phi_{4,3}^{(2)} & \phi_{4,4}^{(2)} & \phi_{4,5}^{(2)} & \phi_{4,6}^{(2)} \\ \phi_{5,1}^{(2)} & \phi_{5,2}^{(2)} & \phi_{5,3}^{(2)} & \phi_{5,4}^{(2)} & \phi_{5,5}^{(2)} & \phi_{5,6}^{(2)} \\ \phi_{6,1}^{(2)} & \phi_{6,2}^{(2)} & \phi_{6,3}^{(2)} & \phi_{6,4}^{(2)} & \phi_{6,5}^{(2)} & \phi_{6,6}^{(2)} \end{bmatrix} \tag{A.2}$$

Diagonal assembling the two substructures to the primitive form gives

$$\mathbf{\Lambda}^p = \begin{bmatrix} \mathbf{\Lambda}^{(1)} & \\ & \mathbf{\Lambda}^{(2)} \end{bmatrix}, \quad \mathbf{\Phi}^p = \begin{bmatrix} \mathbf{\Phi}^{(1)} & \\ & \mathbf{\Phi}^{(2)} \end{bmatrix} \tag{A.3}$$

The node b_1 and node b_2 are constrained to move jointly, i.e., $\overline{x}_4 = \overline{x}_7$, $\overline{x}_5 = \overline{x}_8$, $\overline{x}_6 = \overline{x}_9$, then the constraint matrix $\mathbf{C}$ is formed as

$$\mathbf{C} = \begin{bmatrix} 0 & 0 & 0 & 1 & 0 & 0 & -1 & 0 & 0 & 0 & 0 & 0 \\ 0 & 0 & 0 & 0 & 1 & 0 & 0 & -1 & 0 & 0 & 0 & 0 \\ 0 & 0 & 0 & 0 & 0 & 1 & 0 & 0 & -1 & 0 & 0 & 0 \end{bmatrix} \tag{A.4}$$

With the procedure described in this paper, the eigenvalues and the expanded eigenvectors of the global structure can be obtained as

$$\overline{\mathbf{\Lambda}} = \mathrm{Diag}[\overline{\lambda}_1, \ldots, \overline{\lambda}_9], \quad \overline{\mathbf{\Phi}} = \begin{bmatrix} \overline{\phi}_{1,1} & \cdots & \overline{\phi}_{1,j} & \cdots & \overline{\phi}_{1,9} \\ \vdots & \ddots & & & \\ \overline{\phi}_{i,1} & & \overline{\phi}_{i,j} & & \vdots \\ \vdots & & & \ddots & \\ \overline{\phi}_{12,1} & & \cdots & & \overline{\phi}_{12,9} \end{bmatrix} \tag{A.5}$$

The eigenvalues of the original global structure are equal to $\overline{\Lambda}$ as

$$\mathbf{\Lambda} = \overline{\mathbf{\Lambda}} = \mathrm{Diag}[\overline{\lambda}_1, \ldots, \overline{\lambda}_9] \tag{A.6}$$

The eigenvectors of the original global structure are obtained after discarding the identical values in $\overline{\mathbf{\Phi}}$. For the jth eigenvector,

$$\begin{aligned} \phi_j &= \{\phi_{1,j}, \phi_{2,j}, \phi_{3,j}, \phi_{4,j}, \phi_{5,j}, \phi_{6,j}, \phi_{7,j}, \phi_{8,j}, \phi_{9,j}\}^{\mathrm{T}} = \{\overline{\phi}_{1,j}, \overline{\phi}_{2,j}, \overline{\phi}_{3,j}, \overline{\phi}_{4,j}, \overline{\phi}_{5,j}, \overline{\phi}_{6,j}, \overline{\phi}_{10,j}, \overline{\phi}_{11,j}, \overline{\phi}_{12,j}\}^{\mathrm{T}} \\ &= \{\overline{\phi}_{1,j}, \overline{\phi}_{2,j}, \overline{\phi}_{3,j}, \overline{\phi}_{7,j}, \overline{\phi}_{8,j}, \overline{\phi}_{9,j}, \overline{\phi}_{10,j}, \overline{\phi}_{11,j}, \overline{\phi}_{12,j}\}^{\mathrm{T}} \end{aligned} \tag{A.7}$$

Appendix B. The first- and second-order residual flexibility

For an arbitrary structure with n dofs, $\mathbf{M}$, $\mathbf{K}$, $\mathbf{\Lambda}$, $\mathbf{\Phi}$ represent the mass, stiffness, eigenvalue and eigenvector matrices, respectively. With mass normalization, one has

$$\begin{cases} \mathbf{\Phi}^{\mathrm{T}}\mathbf{M}\mathbf{\Phi} = \mathbf{I}_n \\ \mathbf{\Phi}^{\mathrm{T}}\mathbf{K}\mathbf{\Phi} = \mathbf{\Lambda} \end{cases} \tag{B.1}$$

If the eigensolutions of the structure are divided into m 'master' modes and s 'slave' modes ($m+s=n$) with the same procedure described in this paper, the eigensolutions of the structure can be reassembled as

$$\begin{gathered} \mathbf{\Lambda}_m = \mathrm{Diag}[\lambda_1, \lambda_2, \ldots, \lambda_m] \\ \mathbf{\Phi}_m = [\phi_1, \phi_2, \ldots, \phi_m] \\ \mathbf{\Lambda}_s = \mathrm{Diag}[\lambda_{m+1}, \lambda_{m+2}, \ldots, \lambda_{m+s}] \\ \mathbf{\Phi}_s = [\phi_{m+1}, \phi_{m+2}, \ldots, \phi_{m+s}] \end{gathered} \tag{B.2}$$

Accordingly, the orthogonality relationship satisfies:

$$\begin{cases} \mathbf{\Phi}_m^{\mathrm{T}}\mathbf{M}\mathbf{\Phi}_m = \mathbf{I}_m \\ \mathbf{\Phi}_m^{\mathrm{T}}\mathbf{K}\mathbf{\Phi}_m = \mathbf{\Lambda}_m \end{cases}, \quad \begin{cases} \mathbf{\Phi}_s^{\mathrm{T}}\mathbf{M}\mathbf{\Phi}_s = \mathbf{I}_s \\ \mathbf{\Phi}_s^{\mathrm{T}}\mathbf{K}\mathbf{\Phi}_s = \mathbf{\Lambda}_s \end{cases}, \quad \begin{cases} \mathbf{\Phi}_m^{\mathrm{T}}\mathbf{M}\mathbf{\Phi}_s = \mathbf{0} \\ \mathbf{\Phi}_m^{\mathrm{T}}\mathbf{K}\mathbf{\Phi}_s = \mathbf{0} \end{cases} \tag{B.3}$$

The dynamic flexibility matrix can be transformed as

$$\mathbf{K}^{-1} = [\mathbf{\Phi}_m \;\; \mathbf{\Phi}_s] \begin{bmatrix} \mathbf{\Lambda}_m^{-1} & \mathbf{0} \\ \mathbf{0} & \mathbf{\Lambda}_s^{-1} \end{bmatrix} \begin{bmatrix} \mathbf{\Phi}_m^{\mathrm{T}} \\ \mathbf{\Phi}_s^{\mathrm{T}} \end{bmatrix} = \mathbf{\Phi}_m\mathbf{\Lambda}_m^{-1}\mathbf{\Phi}_m^{\mathrm{T}} + \mathbf{\Phi}_s\mathbf{\Lambda}_s^{-1}\mathbf{\Phi}_s^{\mathrm{T}} \tag{B.4}$$

Therefore,

$$\mathbf{\Phi}_s\mathbf{\Lambda}_s^{-1}\mathbf{\Phi}_s^{\mathrm{T}} = \mathbf{K}^{-1} - \mathbf{\Phi}_m\mathbf{\Lambda}_m^{-1}\mathbf{\Phi}_m^{\mathrm{T}} \tag{B.5}$$

The left item is denoted as the first-order residual flexibility.

When the 'master' eigenvalues contain zero values, an arbitrary small shift ε needs to be introduced usually as $\varepsilon \ll \mathbf{\Lambda}_s$. The first-order residual flexibility can be approximated as

$$\mathbf{\Phi}_s\mathbf{\Lambda}_s^{-1}\mathbf{\Phi}_s^{\mathrm{T}} \cong \mathbf{\Phi}_s(\mathbf{\Lambda}_s + \varepsilon)^{-1}\mathbf{\Phi}_s^{\mathrm{T}} = (\mathbf{K} + \varepsilon\mathbf{M})^{-1} - \mathbf{\Phi}_m(\mathbf{\Lambda}_m + \varepsilon)^{-1}\mathbf{\Phi}_m^{\mathrm{T}} \tag{B.6}$$

Further exploration for the second-order residual flexibility introduces:

$$\begin{aligned} \mathbf{K}^{-1}\mathbf{M}\mathbf{K}^{-1} &= (\mathbf{\Phi}_m\mathbf{\Lambda}_m^{-1}\mathbf{\Phi}_m^{\mathrm{T}} + \mathbf{\Phi}_s\mathbf{\Lambda}_s^{-1}\mathbf{\Phi}_s^{\mathrm{T}})\mathbf{M}(\mathbf{\Phi}_m\mathbf{\Lambda}_m^{-1}\mathbf{\Phi}_m^{\mathrm{T}} + \mathbf{\Phi}_s\mathbf{\Lambda}_s^{-1}\mathbf{\Phi}_s^{\mathrm{T}}) \\ &= \mathbf{\Phi}_m\mathbf{\Lambda}_m^{-1}\mathbf{\Phi}_m^{\mathrm{T}}\mathbf{M}\mathbf{\Phi}_m\mathbf{\Lambda}_m^{-1}\mathbf{\Phi}_m^{\mathrm{T}} + \mathbf{\Phi}_s\mathbf{\Lambda}_s^{-1}\mathbf{\Phi}_s^{\mathrm{T}}\mathbf{M}\mathbf{\Phi}_s\mathbf{\Lambda}_s^{-1}\mathbf{\Phi}_s^{\mathrm{T}} \\ &\quad + \mathbf{\Phi}_s\mathbf{\Lambda}_s^{-1}\mathbf{\Phi}_s^{\mathrm{T}}\mathbf{M}\mathbf{\Phi}_m\mathbf{\Lambda}_m^{-1}\mathbf{\Phi}_m^{\mathrm{T}} + \mathbf{\Phi}_m\mathbf{\Lambda}_m^{-1}\mathbf{\Phi}_m^{\mathrm{T}}\mathbf{M}\mathbf{\Phi}_s\mathbf{\Lambda}_s^{-1}\mathbf{\Phi}_s^{\mathrm{T}} \end{aligned} \tag{B.7}$$

Due to the orthogonality relationship in Eq. (B.3), it is easy to obtain that

$$\mathbf{K}^{-1}\mathbf{M}\mathbf{K}^{-1} = \mathbf{\Phi}_m\mathbf{\Lambda}_m^{-2}\mathbf{\Phi}_m^{\mathrm{T}} + \mathbf{\Phi}_s\mathbf{\Lambda}_s^{-2}\mathbf{\Phi}_s^{\mathrm{T}} \tag{B.8}$$

Therefore, the second-order residual flexibility can be expressed as

$$\mathbf{\Phi}_s\mathbf{\Lambda}_s^{-2}\mathbf{\Phi}_s^{\mathrm{T}} = \mathbf{K}^{-1}\mathbf{M}\mathbf{K}^{-1} - \mathbf{\Phi}_m\mathbf{\Lambda}_m^{-2}\mathbf{\Phi}_m^{\mathrm{T}} \tag{B.9}$$

A small shift ε can be introduced to avoid zero values in $\mathbf{\Lambda}_m$ as

$$\mathbf{\Phi}_s\mathbf{\Lambda}_s^{-2}\mathbf{\Phi}_s^{\mathrm{T}} \cong \mathbf{\Phi}_s[\mathbf{\Lambda}_s + \varepsilon]^{-2}\mathbf{\Phi}_s^{\mathrm{T}} = (\mathbf{K} + \varepsilon\mathbf{M})^{-1}\mathbf{M}(\mathbf{K} + \varepsilon\mathbf{M})^{-1} - \mathbf{\Phi}_m(\mathbf{\Lambda}_m + \varepsilon)_m^{-2}\mathbf{\Phi}_m^{\mathrm{T}} \tag{B.10}$$

The above equations in this appendix are applicable to an arbitrary structure, and thus can be applied to the substructures as employed in the present paper.

References

[1] J.E. Mottershead, M.I. Friswell, Model updating in structural dynamics: a survey, *Journal of Sound and Vibration* 167 (2) (1993) 347–375.

[2] B. Jaishi, W. Ren, Damage detection by finite element model updating using modal flexibility residual, *Journal of Sound and Vibration* 290 (2006) 369–387.

[3] B. Lallemand, P. Level, H. Duveau, B. Mahieux, Eigensolutions sensitivity analysis using a sub-structuring method, *Computer and Structures* 71 (1999) 257–265.

[4] C.G. Koh, B. Hong, C.Y. Liaw, Substructural and progressive structural identification method, *Engineering Structures* 25 (2003) 1551–1563.

[5] H. Kim, M. Cho, Improvement of reduction method combined with sub-domain scheme in large-scale problem, *International Journal for Numerical Methods in Engineering* 70 (2) (2007) 206–251.

[6] D. Choi, H. Kim, M. Cho, Iterative method for dynamic condensation combined with substructuring scheme, *Journal of Sound and Vibration* 317 (1–2) (2008) 199–218.

[7] S. Rubin, Improved component-mode representation for structural dynamic analysis, *AIAA Journal* 8 (1975) 995–1005.

[8] D.J. Rixen, A dual Craig–Bampton method for dynamic substructuring, *Journal of Computational and Applied Mathematics* 168 (2004) 383–391.

[9] R.R. Craig, Coupling of substructures for dynamic analysis: an overview, *Proceedings of 41st AIAA/ASME/ASCE/ASC Structures, Structural Dynamics, and Materials Conference*, Atlanta, GA, 3–8 April 2000, pp. 171–179.

[10] J. Qiu, F.W. Williams, R. Qiu, A new exact substructure method using mixed modes, *Journal of Sound and Vibration* 266 (2003) 737–757.

[11] R.H. MacNeal, A hybrid method of component mode synthesis, *Computers and Structures* 1 (1971) 581–601.

[12] G. Kron, *Diakoptics*, Macdonald and Co., London, 1963.

[13] A. Simpson, B. Tabarrok, On Kron's eigenvalue procedure and related methods of frequency analysis, *Quarterly Journal of Mechanics and Applied Mathematics* 21 (1968) 1039–1048.

[14] A. Simpson, On the solution of $\mathbf{S}(\omega)\mathbf{x} = \mathbf{0}$ by a Newtonian procedure, *Journal of Sound and Vibration* 97 (1) (1984) 153–164.

[15] F.W. Williams, D. Kennedy, Reliable use of determinants to solve non-linear structural eigenvalue problems efficiently, *International Journal for Numerical Methods in Engineering* 26 (1988) 1825–1841.

[16] S. Lui, Kron's method for symmetric eigenvalue problems, *Journal of Computational and Applied Mathematics* 98 (1998) 35–48.

[17] N.S. Sehmi, *Large Order Structural Eigenanalysis Techniques Algorithms for Finite Element Systems*, Ellis Horwood Limited, Chichester, England, 1989.

[18] N.S. Sehmi, The Lanczos algorithm applied to Kron's method, *International Journal for Numerical Methods in Engineering* 23 (1986) 1857–1872.

[19] I W. Mackenzie, Computational Methods for the Eigenvalue Analysis of Large Structures by Component Synthesis, Ph.D. Dissertation, University of London, 1974.

[20] G.L. Turner, Finite Element Modeling and Dynamic Substructuring for Prediction of Diesel Engine Vibration, Ph.D. Dissertation, Loughborough University of Technology, 1983.

[21] A. Simpson, A generalization of Kron's eigenvalue procedure, *Journal of Sound and Vibration* 26 (1973) 129–139.

[22] K.J. Bathe, E.L. Wilson, *Numerical Methods in Finite Element Analysis*, Prentice-Hall, Inc., Englewood Cliffs, NJ, 1989.

[23] A. Simpson, Scanning Kron's determinant, *Quarterly Journal of Mechanics and Applied Mathematics* 27 (1974) 27–43.

[24] W.H. Wittrick, F.W. Williams, A general algorithm for computing natural frequencies of elastic structures, *Quarterly Journal of Mechanics and Applied Mathematics* 24 (1971) 263–284.

[25] Y. Xia, R. Lin, A new iterative order reduction (IOR) method for eigensolutions of large structures, *International Journal for Numerical Methods in Engineering* 59 (2004) 153–172.

[26] K.J. Bathe, *Finite Element Procedures in Engineering Analysis*, Prentice-Hall, Inc., Englewood Cliffs, NJ, 1982.

[27] D.J. Ewins, *Modal Testing: Theory, Practice and Application*, Research Studies Press, Baldock, England, 2000.

[28] Y. Xia, H. Hao, A.J. Deeks, X. Zhu, Condition assessment of shear connectors in slab-girder bridges via vibration measurements, *Journal of Bridge Engineering* 13 (2008) 43–54.